

Michael S.J. Mlynarczyk · Ross L. Sherlock
Anthony E. Williams-Jones

San Rafael, Peru: geology and structure of the worlds richest tin lode

Received: 8 January 2002 / Accepted: 19 August 2002 / Published online: 18 January 2003
© Springer-Verlag 2003

Abstract The San Rafael mine exploits an unusually high grade, lode-type Sn–Cu deposit in the Eastern Cordillera of the Peruvian Central Andes. The lode is centered on a shallow-level, Late Oligocene granitoid stock, which was emplaced into early Paleozoic metasedimentary rocks. It has a known vertical extent exceeding 1,200 m and displays marked vertical primary metal zoning, with copper overlying tin. The tin mineralization occurs mainly as cassiterite–quartz–chlorite veins and as cassiterite in breccias. The bulk of it is hosted by a K-feldspar megacrystic, biotite- and cordierite-bearing leucomonzogranite, which is the most distinctive phase of the pluton. Copper mineralization occurs predominantly in the veins that straddle the metasedimentary rock–intrusion contact or are hosted entirely by slates. Both tin and copper mineralization are associated with strong chloritic alteration, which is superimposed on an earlier episode of sericitization and tourmaline–quartz veining. Based on the distribution of alteration and ore mineralogy, cassiterite deposition and subsequent chalcopyrite precipitation are believed to have been the result of a single, prolonged hydrothermal event. The source of the metals is inferred to be a highly evolved, peraluminous magma, related to the leucomonzogranitic phase of the San Rafael pluton. Preliminary fluid inclusion microthermometry suggests that ore deposition took place during the mixing of moderate and low salinity fluids, which were introduced in a series

of pulses. Several large fault-jogs, created by sinistral-normal, strike-slip movement, are interpreted to have focused synkinematic magmatic fluids and permitted their effective mixing with meteoric waters. It is proposed that this mixing led to rapid oxidation of Sn (II) chloride species and caused supersaturation of the fluids in cassiterite, resulting in the development of localized, high-grade ore shoots. A favorable structural regime that promoted large-scale mixing of two fluids originating under very different physico-chemical conditions appears to have been the key factor responsible for the unusual richness of the deposit.

Keywords Cassiterite · Chloritization · Cu–Sn zoning · Fluid mixing · Lode deposit

Introduction

San Rafael is a lode-type cassiterite–sulfide deposit, located in the northernmost extension of the Central Andean tin belt, in the department of Puno, southeastern Peru (Fig. 1). It crops out at elevations between 4,500 and 5,100 m, on the flanks of the glacier-capped Quenamari Mountain (Fig. 2a, b). The mine is owned and operated by Minsur S.A., and has been worked for more than 40 years.

The deposit occurs in a NW-trending and NE-dipping composite vein system, spatially associated with a Late Oligocene (~25 Ma) granitoid intrusion. Although there are numerous subparallel veins in the district, a single complex vein, the San Rafael lode, hosts the bulk of the known mineralization, which is of unusually high grade. It is estimated that, prior to mining activity, the deposit had an average tin grade of 4.7 wt%, and a total resource of ~1 million tonnes (t) Sn (metal), making it the highest grade primary tin deposit in the world (Fig. 3). Proven and probable reserves are estimated at 13.9 million t ore, grading 5.27 wt% Sn and 0.16 wt% Cu (Minsur, unpublished data, December 2000). Mining and processing of the ores has increased steadily from

Editorial handling: N. White

M.S.J. Mlynarczyk (✉) · A.E. Williams-Jones
McGill University, Department of Earth and Planetary Sciences,
3450 University St., H3A 2A7 Montreal, Quebec, Canada
E-mail: michael@eps.mcgill.ca

R.L. Sherlock
SRK Consulting, Suite 800, 580 Hornby St.,
Vancouver, BC V6C 3B6, Canada

Present address: R.L. Sherlock
Canada-Nunavut Geoscience Office,
P.O. Box 2319 Iqaluit, Nunavut X0A 0H0, Canada



Fig. 1 Location of the San Rafael Sn–Cu deposit in the Central Andean tin belt (outline and dots representing the deposits are modified after Lehmann 1979; Claire and Minaya 1979)

500 t/day in 1980 to 2,500 t/day in 1999. Present production of 27,000 t/year of tin metal represents ~13% of the annual hard-rock production of tin globally (J. Carlin, USGS, written communication 2000).

Exploration and mining history

The exploration history of the San Rafael area dates back to 1913, when a German–Chilean company discovered copper mineralization on the northwestern slopes of Quenamari Mountain, which at the time was largely covered by glaciers (Arenas 1980a, 1999). In 1947, prospector Rafael Avendaño outlined a copper deposit, which was subsequently named the San Rafael lode. Development of the near surface, high-grade copper mineralization commenced in 1958 when Lampa Mining Co. used the copper ore to blend with copper–silver ore from the nearby Berengueta deposit. In 1966, W.R. Grace & Co. purchased 67% of Lampa Mining Co. and formed Minsur Sociedad de Responsabilidad Ltda. The company operated the deposit until 1977, when the Brescia Group purchased Minsur and Lampa's shares, becoming 100% owners and operators of San Rafael, as Minsur Sociedad Anonima.

During the initial period of development, mining was focused mainly on the near-surface copper orebody, as the underlying tin ore had not been discovered. In the late 1970s, copper grades were decreasing and the known mineralization was thought to terminate at about the 4,533-m level (Arenas 1999). However, exploration and development work undertaken by Minsur S.A. in 1980 led to

the discovery of several large tin orebodies grading as much as 15 wt% Sn, below the 4,533-m elevation. Continuing exploration has demonstrated the presence of high-grade tin ore down to the 3,950-m level.

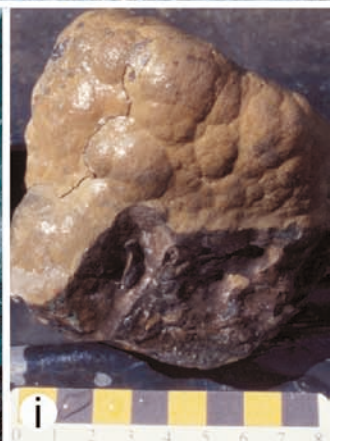
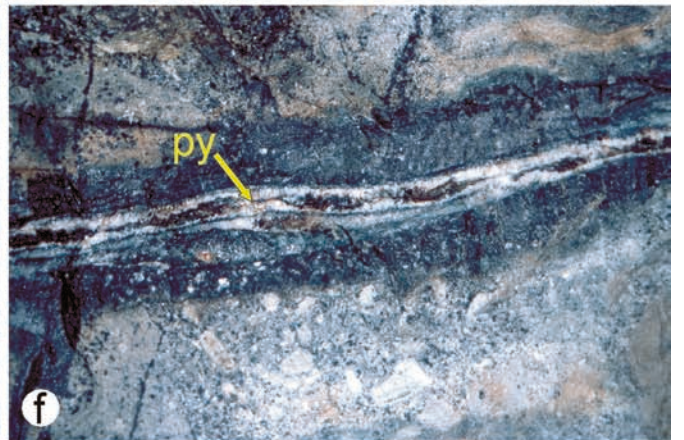
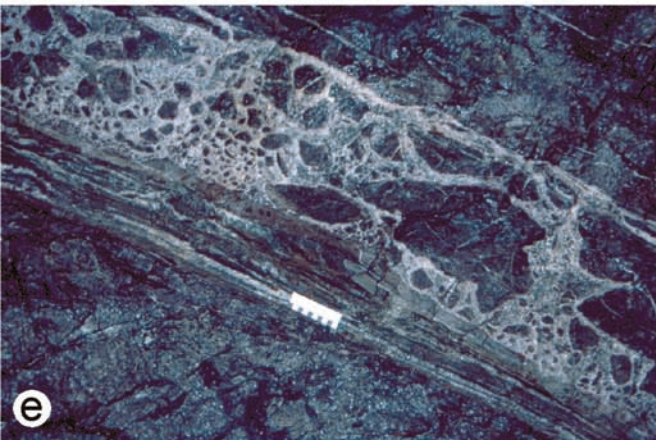
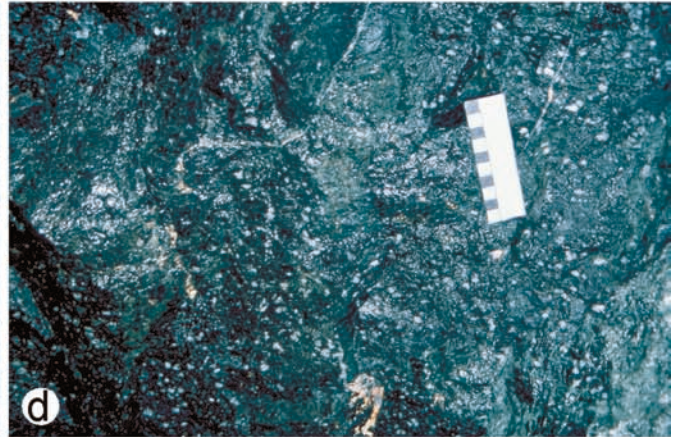
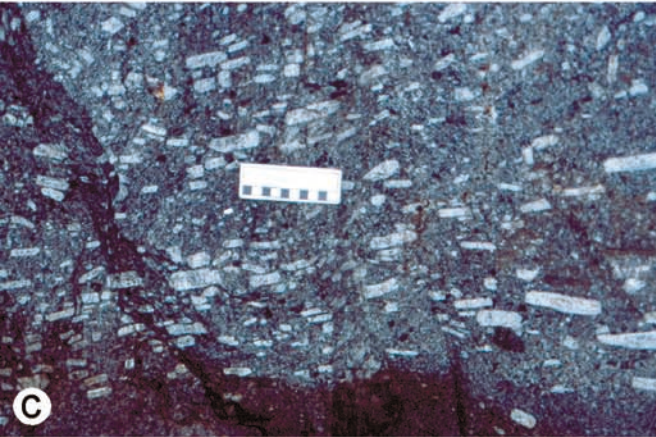
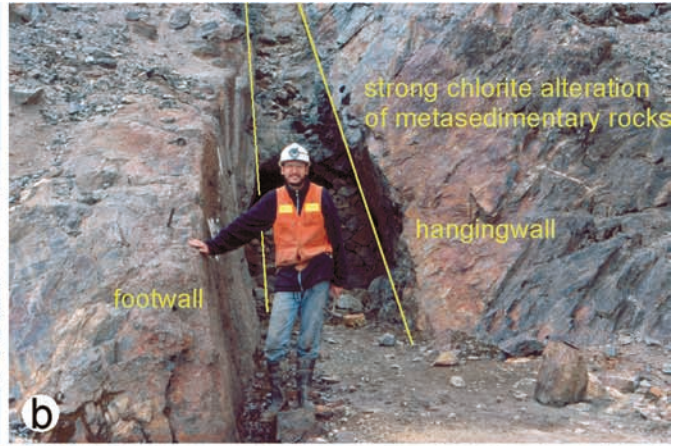
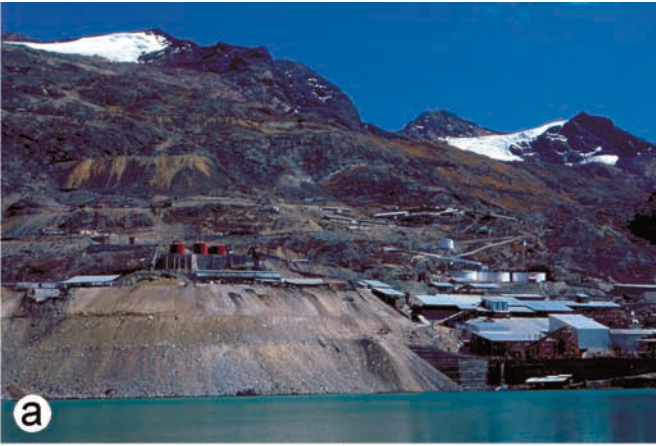
Regional geological setting

The San Rafael property lies within the Cordillera Carabaya of Peru, part of the Eastern Cordillera, which consists mainly of a thick sequence of marine sedimentary rocks. Throughout the Phanerozoic, this region underwent convergent plate interaction, orogeny and intermittent, mixed, mantle- and crust-derived bimodal magmatism (Clark et al. 1990). The stratigraphy of the area, described in detail by Laubacher (1978) and Kontak and Clark (1988), is shown schematically in Fig. 4. The lower 10–15 km of the sequence is composed of early Paleozoic pelites and psammites (the San José, Sandía and Ananea Formations), which are inferred to overlie unexposed Precambrian gneissic basement. The early Paleozoic strata were deformed and metamorphosed to sub-greenschist facies in a Late Devonian–Early Carboniferous orogeny.

These rocks are unconformably overlain by a 3- to 4-km-thick succession of late Paleozoic psammites and carbonates (Mississippian Ambo Group, Pennsylvanian Tarma Group, and Permian Copacabana Group). Following a weak episode of deformation that lacked accompanying regional metamorphism, there was further sedimentation and intermittent alkaline volcanism from mid-Permian to Triassic times, which led to the accumulation of approximately 3 km of red beds and intercalated volcanic rocks (Mitu Group). The sequence is unconformably capped by ~1 km of Cretaceous psammites and carbonates (Cotacucho Group) and approximately 800 m of Miocene–Pliocene felsic ignimbrites and red beds of the Crucero Supergroup (Clark et al. 1983; Kontak et al. 1995; Sandeman et al. 1996).

Plutonic rocks were emplaced repeatedly from the Late Devonian to the late Tertiary. These intrusions can be broadly

Fig. 2a–i Geological setting: alteration and vein styles. **a** View of the San Rafael mine. Glacier fields in the background are on the left: Nevado San Bartolome de Quenamari (5,299 m) and on the right: Nevado San Francisco de Quenamari (5,297 m). The present entrance to the mine (at 4,533 m) and the mine plant are in the lower right part of the photograph, beside lake Chocñacota (4,500 m). Old waste dumps can be seen in the middle left part of the photograph. **b** The San Rafael lode at the entrance of the 4,820-m adit. **c** Porphyritic granitoid on the 4,200-m level, containing large, flow-oriented alkali-feldspar megacrysts. The scale is in centimeters. **d** Strong, pervasive chloritization of the granitic wall rock on the 4,225-m level of the Ore Shoot. The only primary mineral remaining is quartz, visible as small white patches in the green groundmass. The scale is in centimeters. **e** Barren, quartz-cemented 'breccia-dyke' of angular wall rock fragments, hosted by tourmalinized wall rock on the 4,225-m level of the Ore Shoot. The scale is in centimeters. **f** The Jorge vein as seen in the roof of the 4,050-m level. After an early stage of sericitization (best seen in the upper part of the photograph) and tourmalinization (along the vein margins), the vein was repeatedly opened and filled with quartz, chlorite, and sulfides (mostly pyrite, see arrow). The vein width is ~25 cm (including the tourmalinization envelope). **g** Subvertical cassiterite–quartz–chlorite vein crosscutting early tourmaline–quartz veins on the 4,310-m level of the Ore Shoot. Note the intense chloritic haloes around the quartz veins in the lower central part of the photograph. The scale is in centimeters. **h** Late, barren quartz vein crosscutting the subvertical cassiterite–quartz–chlorite vein shown in **g**. The scale is in centimeters. **i** Botryoidal tin ore from the mined-out zone of wood tin ores at an elevation of ~4,450–4,500 m. The scale is in centimeters. The wood tin ores at San Rafael represent the bulk of the wood tin known in the world (A.H. Clark, personal communication)



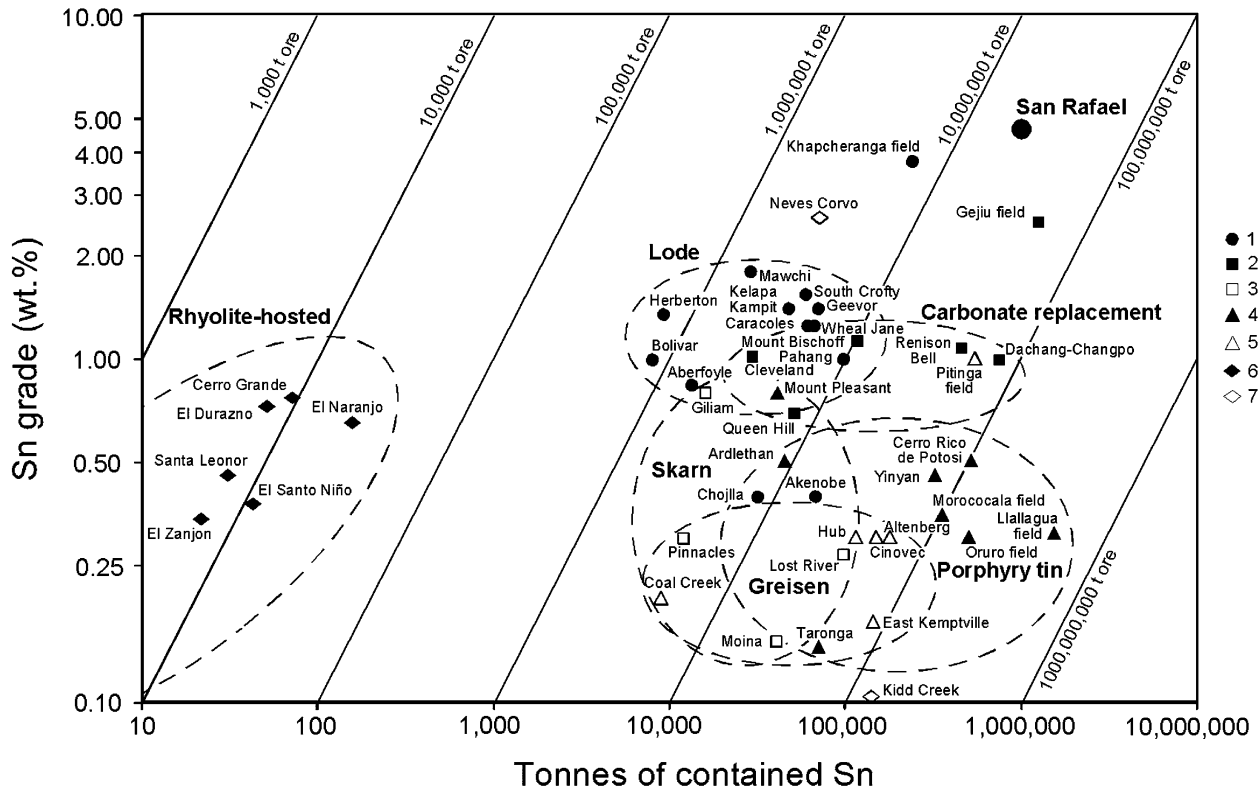


Fig. 3 Grade versus tonnage for selected, large and high-grade, primary tin deposits. The deposit types are 1 lode, 2 carbonate replacement, 3 skarn, 4 porphyry, 5 greisen, 6 rhyolite-hosted (Mexican type), 7 VMS. Some deposits belong to more than one class. The outline of the circles is schematic. Data compiled from Evans 1993; Singer et al. 1993; Kirkham and Sinclair 1995; Sinclair 1995; P Laznicka, personal communication 2000; Minsur, unpublished data

subdivided into Late Devonian–Early Carboniferous granitoids with minor Sn–W mineralization; large Permo-Triassic granitoid batholiths with significant Sn–Cu–W–Mo mineralization; small Late Cretaceous granodiorite stocks with minor silver and base metal mineralization; and stocks of middle to late Tertiary granitic rocks, which host the bulk of the Sn–W–Ag–base metal mineralization in the area, including the San Rafael deposit (Kontak and Clark 1988).

The Late Oligocene (~25 Ma; Clark et al. 1983) granitoid intrusion, with which the San Rafael deposit is associated, is part of the Picotani intrusive suite, belonging to the Crucero Supergroup (Sandeman et al. 1995, 1996). Sandeman et al. (1995, 1996) suggested that the Nazca plate ruptured in the vicinity of the Peru–Chile trench at about 38 Ma, and the foundering of the downgoing slab resulted in the formation of a slab window. This, in turn, caused an episode of anomalous asthenospheric upflow, which was responsible for the emplacement of rocks of the Picotani Group between 25 and 22 Ma. A local transtensional stress regime permitted the ascent of voluminous, mantle-derived mafic melts into the middle crust, which induced dehydration, partial melting of metasedimentary rocks (metapelites) and generation of water-undersaturated peraluminous felsic melts. The mixing and co-mingling of parental and daughter melts in shallow magma chambers gave rise to a diversified igneous suite, comprising mantle-derived shoshonites, minettes, absarokites, high-K calc-alkaline basalts, and peraluminous rhyodacites and monzogranites (Sandeman et al. 1995). Tin mineralization is spatially associated with strongly peraluminous leucomonzogranites, which crop out in only a few localities, such as San Rafael and the nearby Santo Domingo tin prospect.

Geology of the San Rafael district

The San Rafael area is underlain mainly by slates and subordinate quartzites of the Late Ordovician Sandía Formation, which were intruded in the Late Oligocene by a small (<15 km²) plug of K-feldspar megacrystic granitoid porphyry (Fig. 2c). The pluton is elongated to the northeast, and although its core corresponds to a prominent topographic high (5,300 m), much of the pluton remains unroofed. The surface exposure of the intrusion is limited to two stocks, each a few hundred meters in diameter, which converge at a depth of less than 1 km below the surface. Numerous NW-trending dykes of granitoid porphyry, and several that are semi-annular, crop out in the area surrounding the two stocks.

The metasedimentary rocks hosting the intrusion form a structural dome, which consists of a core of early Paleozoic rocks belonging to the Sandía, San José and Ananea Formations, surrounded by late Paleozoic rocks of the Ambo, Tarma and Copacabana Groups. Strata of the Sandía Formation are marked by a strong penetrative foliation, generally parallel to bedding, and are strongly deformed in a series of recumbent to upright folds and associated thrust faults. The early Paleozoic metasedimentary rocks immediately surrounding and overlying the intrusion have undergone contact metamorphism, indurating and locally converting them to hornfels.

Granitic rocks forming the San Rafael pluton can be subdivided into two major phases: a white-gray,

	Age (Ma)	System	Cordillera Carabaya	Ore event	Formation (Fm.) / Group (Gr.), lithology and thickness
CENOZOIC	1.6	Quaternary	Hiatus	U	Glacial and alluvial deposits, areally restricted mafic volcanic rocks Quenamari Gr. felsic volcanic rocks, red beds } Crucero Supergroup Picotani Gr. mafic-felsic volcanic rocks, red beds } (< 800 m)
		Tertiary		Sn-W Ag-BM	
	65	Cretaceous	Hiatus	Ag-BM	
MESOZOIC	145	Jurassic	Hiatus		Vilquechico Fm. shales Cotacucho Gr. sandstones, shales, dolomites (< 1,100 m)
	200	Triassic		Ag-Cu	Allinccapác Gr. peralkaline volcanic rocks
	251	Permian		W-Sn Mo-Cu	Mitu Gr. alkaline volcanic rocks and red beds (< 3,000 m)
	300	Carboniferous			Tarma-Copacabana Gr. limestones, sandstones, shales (< 3,000 m) Ambo Gr. sandstones and shales (> 1,500 m)
PALEOZOIC	355	Devonian	Hiatus	Sn-W	Ananea Fm. shales (> 2,500 m)
	418	Silurian	Hiatus		Sandía Fm. shales and quartzites (~ 3,500 m)
	441	Ordovician			San José Fm. shales (> 3,500 m)

Fig. 4 Schematic lithostratigraphic column for the Cordillera Carabaya, indicating of the major metallogenic episodes (modified after Clark et al. 1983, 1990; Kontak et al. 1986, 1990; Kontak and Clark 1988; Sandeman et al. 1995, 1996). Time scale from Okulitch 1999. The size of the symbols representing the intrusions, as well as the font of the corresponding mineralization (BM refers to base metals), are proportional to the importance of the magmatic/metallogenic event

porphyritic leucomonzogranite, and a dark-gray, fine-grained to porphyritic granodiorite. The most distinctive phase is a coarse-grained, biotite- and cordierite-bearing subsolvus leucomonzogranite with abundant alkali feldspar megacrysts, ≤ 10 cm in length. This phase has a strongly peraluminous character, as indicated by the presence of cordierite, and may be classified as an S-type granite, as defined by Chappell and White (1974). Granodiorites, which contain cordierite, garnet, and minor sillimanite, are also S-type and increase in volume at depth. Finally, some tonalite enclaves occur locally in the granodiorites and leucogranites.

The San Rafael area hosts a number of subparallel, generally NW-trending and moderately to steeply dipping, planar veins (Fig. 5). These veins cut the intrusion–metasedimentary rock contacts without any appreciable deflection, and can be traced on surface for > 3 km. Within the slates of the Sandía Formation, the vein traces are commonly marked by zones a few meters in width of anastomosing milky quartz veinlets containing minor amounts of sulfide minerals and surrounded by chloritization haloes. Locally, the veinlets coalesce into quartz–sulfide lenses that are tens of centimeters wide and several meters or tens of meters long. At depth, within the granitoid porphyry, the veins are more regular in form and average from 0.5 to 1.5 m in width.

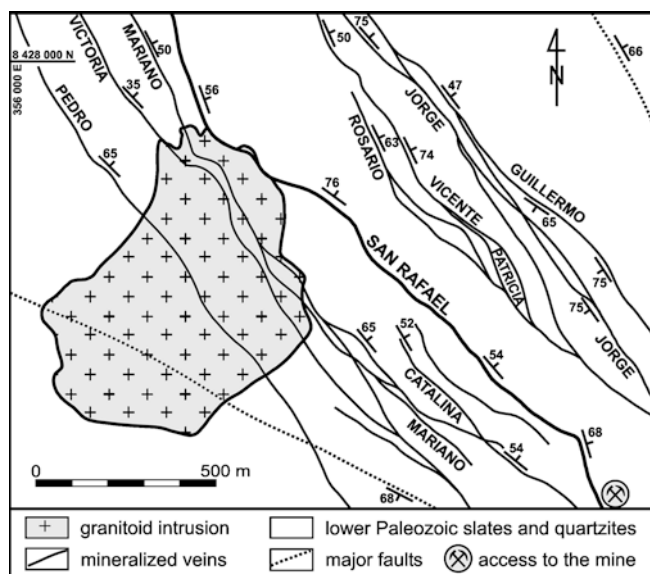


Fig. 5 Bedrock geology of the southwestern part of the San Rafael district (modified after Arenas 1980b; Sherlock 1999). The stock shown is composed of granite and granodiorite and is one of the two exposures of the San Rafael pluton (the other lies outside the map area, in the northeastern part of the district)

Geology and structure of the San Rafael lode

Structural geology

The San Rafael vein, referred to as lode because of its structural complexity, on average, strikes $\sim 330^\circ$, dips 40 to 75° to the northeast and can be traced on surface for a distance of ~ 3.5 km. It is mineralized over an unusually

large vertical extent, exceeding 1,200 m (5,100–3,900 m above sea level), and hosts ~98% of the tin reserves of the San Rafael deposit (Minsur, unpublished data 1999). The width of the vein is <2 m in the upper part of the deposit (Fig. 2b), but, at depth, the structure dilates into a series of subvertical shoots, some of which are as much as 50 m wide (Figs. 6 and 7). Field observations show that there was movement along the San Rafael fault synchronous with vein filling. Kinematic indicators, such as fault-vein relationships, drag folds, and stratigraphic offsets, consistently indicate a normal–sinistral sense of displacement (Sherlock 1999). Slickensides are poorly developed, but where seen are steeply plunging.

The surface expression of the San Rafael lode consists of a 1- to 2-m-wide network of anastomosing quartz

veinlets and quartz-cemented breccias, surrounded on both sides by a zone of chloritization that is ~20 m wide. The lode is planar (striking 328° and dipping 65°, on average, Fig. 8a) and its hanging wall and foot wall contacts are delimited by narrow (~2 cm), gouge-filled fault breccias. Mineralization consists of narrow, semi-continuous bands of massive chalcopyrite, generally developed along the hanging wall and foot wall contacts.

The lode continues to be planar and narrow (<2 m) down to the 4,600-m level (striking 332° and dipping 68°, on average, Fig. 8b), and displays a geometry identical to that of the surface exposures. It generally has sharp contacts with the adjacent unmineralized wall rock, is commonly brecciated, and exhibits extensive textural evidence of open-space filling. The mineralization consists of narrow zones (~20 cm wide) of massive to semi-massive chalcopyrite with minor cassiterite.

Below the 4,533-m level, two major fault jogs are developed, producing an important change in the style of mineralization (Figs. 6 and 7). These jogs localize

Fig. 6 **a** Longitudinal section of the San Rafael lode (modified after Minsur, unpublished data). Mine levels correspond to the elevation. **b** Cross section of the San Rafael lode through the Contact Orebody (N 58 E)

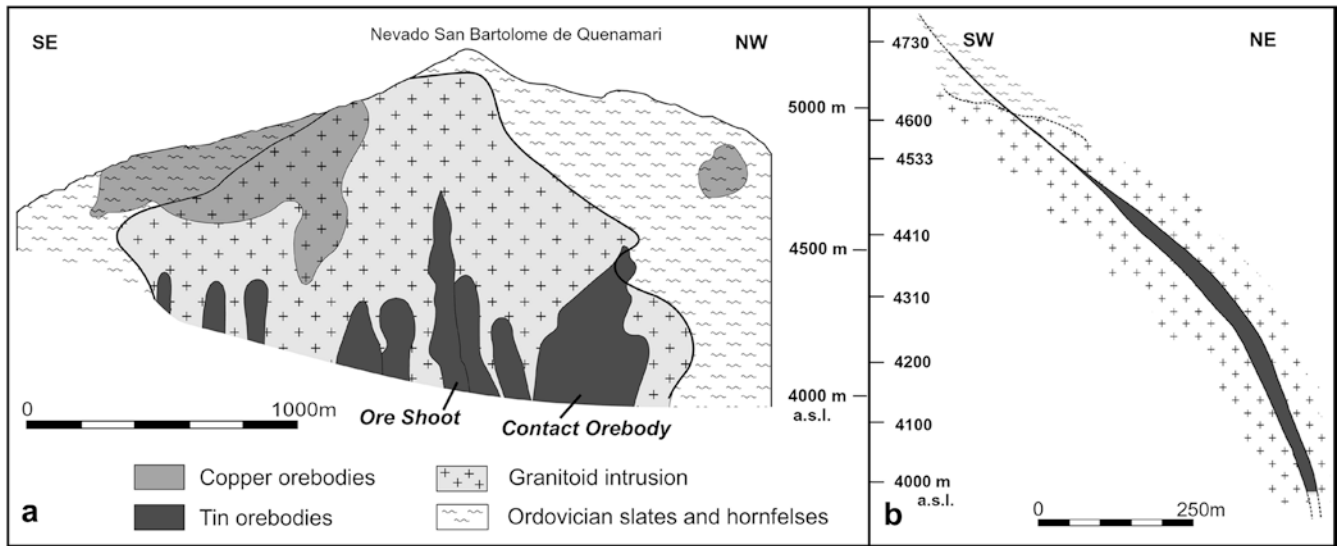


Fig. 7 Structural contours on the San Rafael lode and intrusion-metasedimentary rock contact (modified after Sherlock 1999; Minsur, unpublished data)

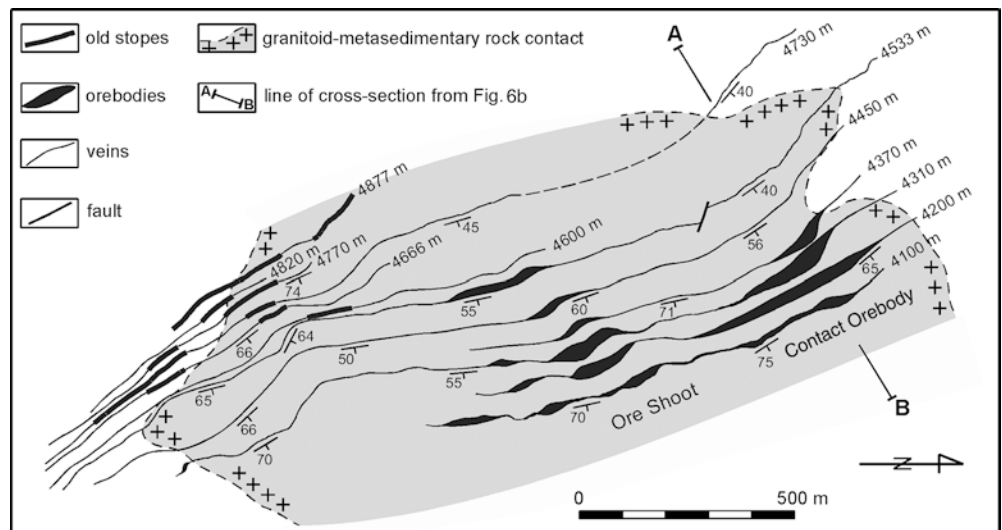
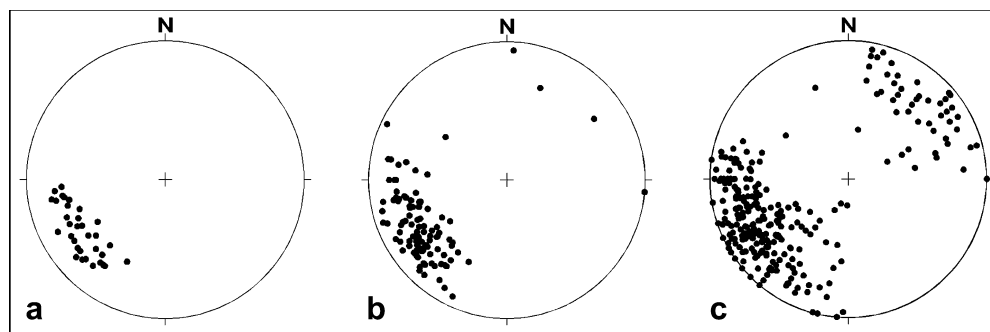


Fig. 8 Stereonet plots of the main- and late-stage veins composing the San Rafael lode, as exposed **a** on the surface ($n=33$), **b** between the surface and the 4,600-m level ($n=108$), **c** between the 4,533- and the 4,050-m levels ($n=301$). The data are plotted on the lower hemisphere, as poles to the plane in an equal area projection



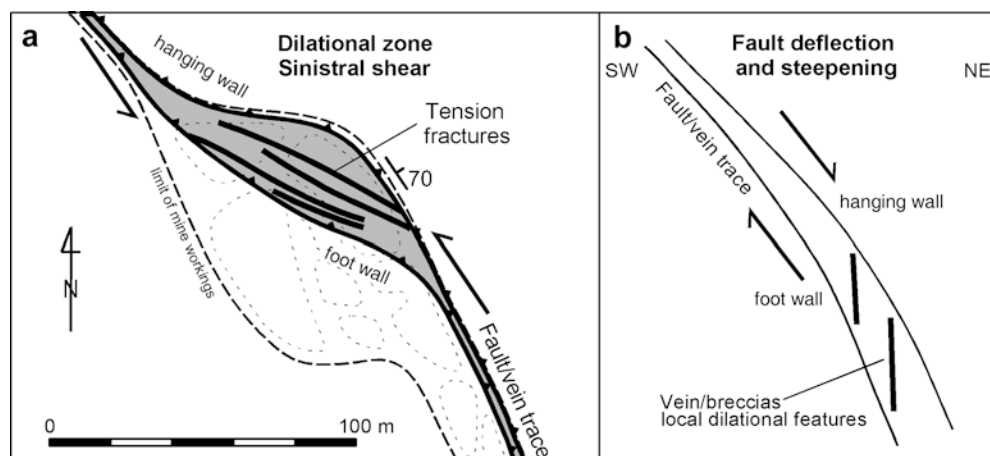
dilational zones, where the sinistral–normal San Rafael fault has stepped to the west and steepened (Fig. 9). The jogs widen considerably at depth (up to ~ 50 m) and form the Ore Shoot and Contact orebodies, elongated sinuous zones, marked by sharp hanging wall and foot wall contacts, and characterized by an abundance of NW-striking (Fig. 8c), cassiterite-mineralized quartz veins and breccia zones. The two orebodies display a similar style of mineralization and host the highest concentration of cassiterite in the deposit. There are also several smaller orebodies at depth, which include the South Contact, Breccia 150-S, Ramp 410, 150, 310-S, and 250-S orebodies. Significantly, all the orebodies in the lower part of the lode are confined to the granitoid intrusion (Figs. 6 and 7), and the veins become irregular where they are hosted by the sedimentary rocks.

Cassiterite associated with quartz and chlorite dominates the lower part of the lode. It occurs mainly as open fracture-filling, breccia and replacement bodies (Figs. 2g–i and 10a–e), as well as disseminations in strongly chloritized wall rock (Fig. 2d). Repeated opening of the veins, evident from crack and fill textures, as well as multiple episodes of brecciation, produced a very complex lode morphology (Fig. 2e, f). Cassiterite is most abundant where veins branch and intersect or where they deflect in strike or dip. The highest ore grades (as much as 45 wt% Sn) occur in breccias that form zones several meters wide, and in the major veins in the foot wall and hanging wall of the lode structure.

The veins composing the San Rafael lode have been subdivided, based on their mineralogy (Fig. 11). Cross-cutting relationships among the different vein types clearly demonstrate that the oldest veins are tourmaline- and quartz-bearing (Fig. 2f, g). These veins form a conjugate set (one set striking $\sim 330^\circ$ and NE-dipping, the other striking $\sim 295^\circ$ and SW-dipping). By contrast, all main- (ore) and late-stage (post-ore) veins have the same general orientation (strike $\sim 330^\circ$ and dip NE).

Surface geological mapping identified tourmaline–quartz veins orthogonal to the San Rafael lode, occupying dilational zones in thrust faults that have been subsequently cut and offset by the lode. These tourmaline–quartz veins are, therefore, very early and may be unrelated to the tin–copper mineralization. However, underground mapping showed that there are major tourmaline–quartz veins, and volumetrically important tourmaline–quartz breccia dykes (described below), which are concordant with the strike of the San Rafael vein–breccia system. Some of these veins were subsequently reopened and filled by the main- and late-stage veins (Fig. 2f). It is thus possible that there was more than one generation of tourmaline-bearing veins and tourmaline crystallization could have partly overlapped tin deposition. Tourmaline–quartz veins and breccias have, therefore, been included in the early paragenesis of the lode, and a genetic link between these and the younger tin- and copper-bearing veins is tentatively inferred.

Fig. 9 Schematic diagram of the Contact Orebody, showing the relative positions of the fault/vein traces, hanging wall and foot wall contacts, and the geometry of the vein/breccia system that comprises the orebody in relation to the sinistral normal displacement on the fault. **a** Plan view on the 4,370-m level. **b** Vertical section (not to scale)



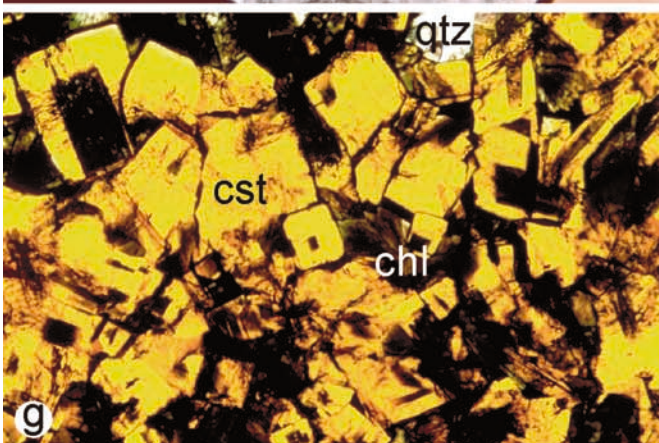
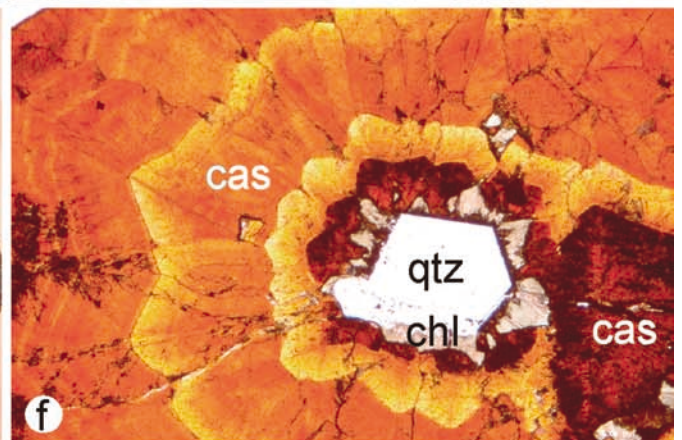
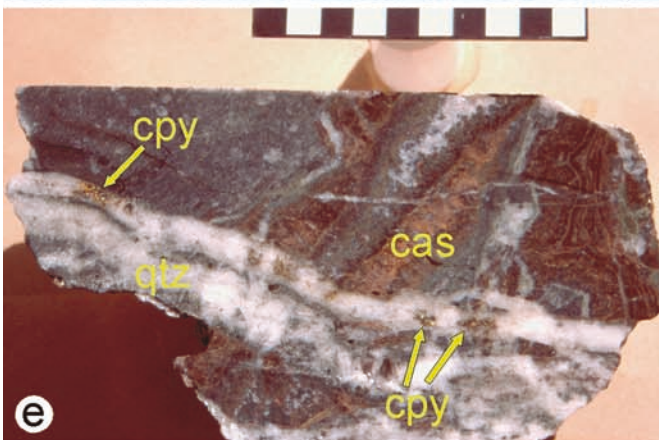
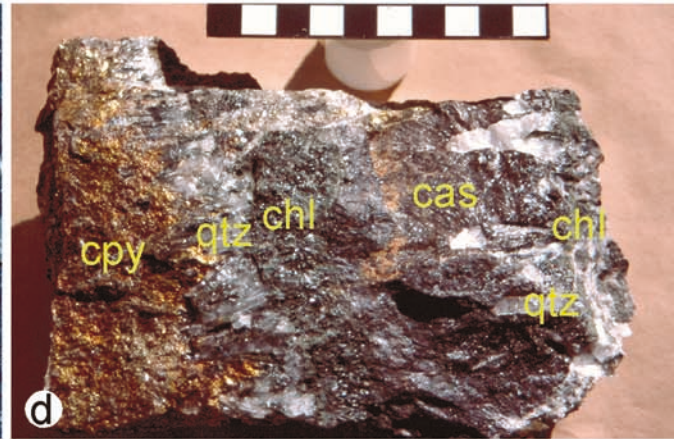
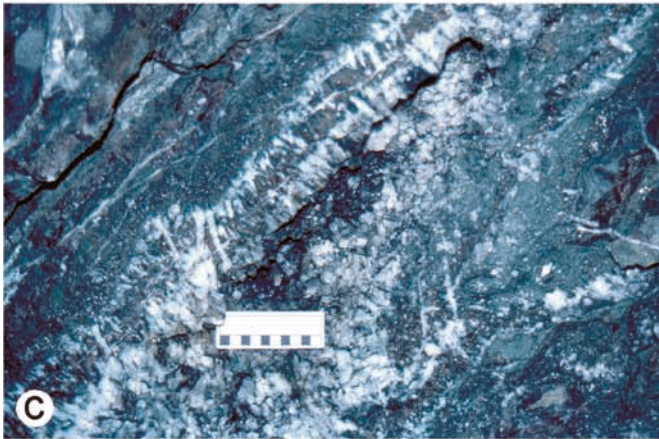
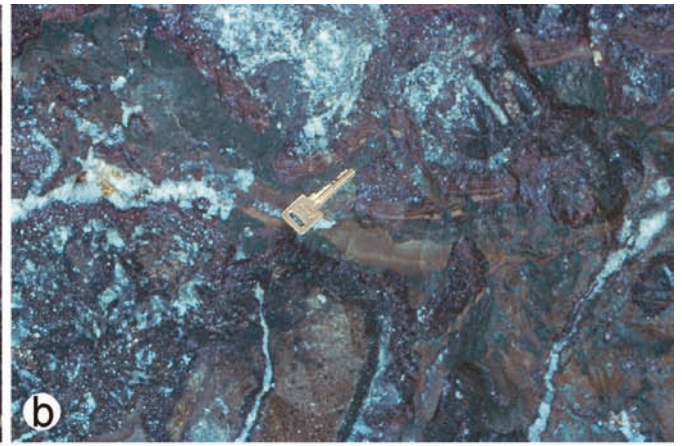
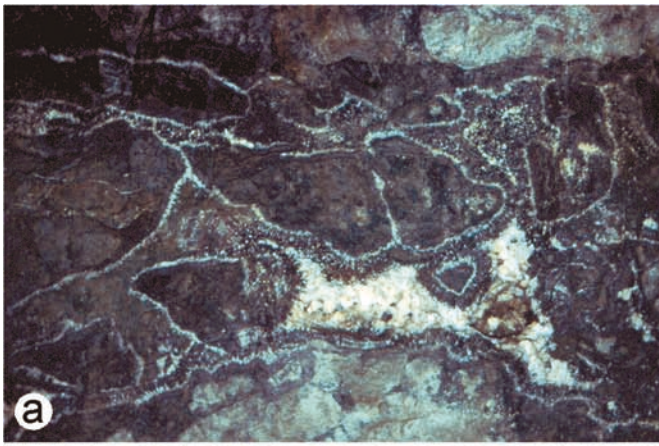




Fig. 10a–h Ore textures and paragenetic relationships. **a** Cassiterite-bearing breccia-dyke in the roof of the 4,225-m level of the Contact Orebody. Sub-angular fragments of chloritized wall rock are overgrown by quartz, cassiterite, and chlorite and the remaining space is filled with milky quartz, locally forming quartz vugs. Vein width is ~40 cm. **b** Fragments of broken layers of wood tin (yellow-brown) and chlorite (green) in a wall rock composed mostly of massive cassiterite (dark brown), quartz, and chlorite. Ore Shoot, 4,330-m level. **c** Cassiterite–quartz–chlorite vein on level 4,270 m of the Contact Orebody. Note the cockscomb structure and the alternating layers of quartz, chlorite, and cassiterite. The scale is in centimeters. **d** Fragment of a composite cassiterite–quartz–chlorite–sulfide vein from the 4,310-m level of the Contact Orebody. The massive cassiterite (*cas*), associated with quartz (*qtz*), and chlorite (*chl*) is close to the vein selvage, whereas the sulfides, i.e., chalcopyrite (*cpy*) and minor pyrite form the center of the vein (sample SAR-R103). The scale is in centimeters. **e** Banded veins of massive cassiterite (*cas*), crosscut by quartz veins (*qtz*) bearing chalcopyrite (*cpy*). The sample was taken on level 4,100 m of the “150” orebody (sample SAR-A4). The scale is in centimeters. **f** Botryoidal cassiterite ore (of the type shown in Fig. 2i) in thin section, plane polarized light. The sequence starts with quartz (*qtz*), which is overgrown by minor chlorite (*chl*) and cassiterite (*cas*) displaying color zoning from dark brown to yellow (sample SAR-D5). Width of photo: 2 mm. **g** Needle tin ore in a doubly polished section (40 μm), plane polarized light. The square habit of the cassiterite crystals (*cas*) is apparent and arises from them being viewed in a section perpendicular to their elongation. Fibrous aggregates of chlorite (*chl*) and quartz grains (*qtz*) are interstitial to the cassiterite (sample SAR-R85). Width of photo: 2 mm. **h** Needle tin ore in a doubly polished section (200 μm), showing acicular crystals of cassiterite (*cas*), pale green chlorite (*chl*), and quartz (*qtz*) in plane polarized light (sample SAR-R119). Width of photo: 2 mm

Alteration and veining

Several distinct stages of alteration and veining accompanied the development of the San Rafael lode and are briefly described below, in chronological order, as inferred from paragenetic relationships. They have been grouped into four broad stages, following the subdivision proposed by Palma (1981).

Stage I (early, pre-ore)

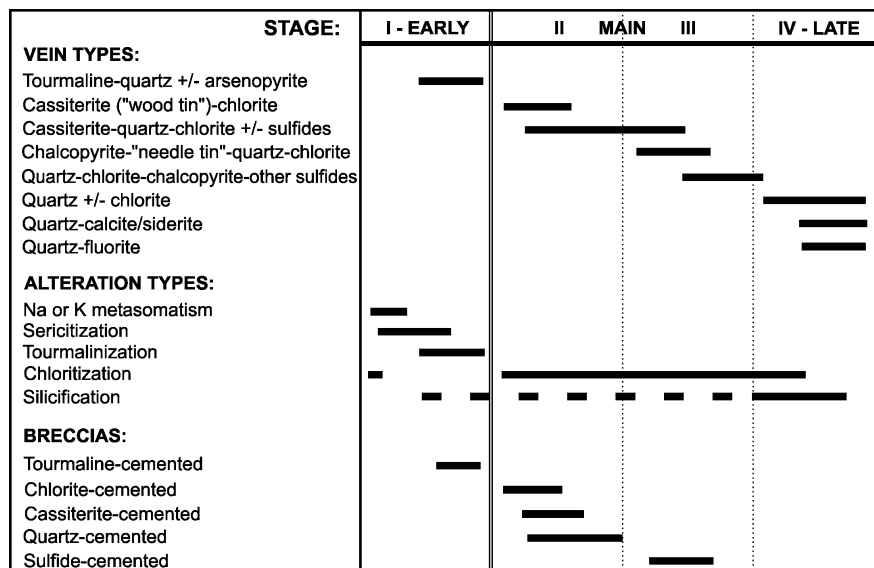
The earliest alteration is sodic-potassic and is manifested by conspicuous overgrowths of hydrothermal albite or orthoclase on pre-existing feldspars (referred to as pseudo-rapakivi textures by Kontak and Clark 1988). This early alteration is observed only locally within the granitoid intrusion and its irregular distribution is further obscured by the overprint of subsequent alteration.

In contrast to sodic-potassic metasomatism, all other pre-ore alteration is clearly associated with tourmaline–quartz veins. These early veins are very common and, in addition to schörl–dravite tourmaline and quartz, also contain arsenopyrite, but are in general barren of cassiterite. Typically, they are surrounded by envelopes of pervasive sericitization that are 1 to 30 cm wide (Fig. 2f, g). Where these veins form denser stockworks, sericitic alteration occurs over a width of many meters, but its original extent is commonly obscured by main-stage alteration. In addition to the ubiquitous sericitic haloes, the alteration envelopes of some tourmaline–quartz veins also display an outer zone of very weak, early chloritization and a 0.5- to 5-cm-wide inner zone of tourmalinization.

Fracture-controlled, pervasive tourmalinization of the wall rock post-dated sericitization and is commonly associated with silicification. This alteration can attain a width of tens of centimeters and normally preserves only relics of the quartz phenocrysts from the original granitoid (Fig. 2e) and, in places, the outlines of tourmalinized K-feldspar phenocrysts.

Finally, much and perhaps the bulk of the tourmaline in the San Rafael lode occurs within numerous, sub-vertical, tourmaline–quartz breccia dykes, which locally are many meters in width and follow the lode along strike for hundreds of meters. These extremely fine-grained microbreccias are composed mainly of fragments of quartz or tourmalinized wall rock, embedded

Fig. 11 Simplified paragenesis for the San Rafael deposit



in a matrix of pervasively tourmalinized rock flour. Generally, they are heavily veined by quartz.

Stage II (main ore stage-A)

The bulk of the tin at San Rafael was deposited as botryoidal wood tin (Figs. 2i and 10b, f) and as veins or breccias consisting almost entirely of quartz, chlorite, and cassiterite (Figs. 2g, h and 10a, c). Strong and pervasive, texturally destructive chloritization accompanied the tin mineralization and affected the entire lode structure for distances varying from < 1 to > 10 m on either side of the vein system, in both the intrusion and the surrounding metasedimentary rocks. Chlorite completely replaced cordierite, biotite, and feldspars (leaving only the quartz phenocrysts), and produced a dark-green rock with scattered patches of clear to milky quartz (Fig. 2d, g). Rocks previously sericitized were also converted to chlorite, but tourmalinized rocks were left unaffected.

Stage III (main ore stage-B)

Sulfide mineral deposition occurred mainly during Stage III and is represented by quartz–chlorite–chalcopyrite–sphalerite–galena–cassiterite (\pm other sulfides) veins. Cassiterite is present as fine-grained needles and prisms (Fig. 10g, h) in contrast to its massive or botryoidal form in stage II. Wall-rock alteration is extensive and similar to that of stage II, with a chloritic halo extending for as much as several meters from the surface expression of the copper-bearing veins. The distinction between stage II and III veins is based on crosscutting relationships (Fig. 10e), mineralogy, and metal content.

Stage IV (late, post-ore)

The large (as wide as 1 m), post-ore, quartz (\pm calcite, siderite or fluorite) veins of stage IV are essentially barren and contain only traces of chalcopyrite and other sulfide minerals (Fig. 2h). They are bordered by narrow zones of intense chloritic alteration, which macroscopically resembles that of the main ore stages. Locally, the chloritized wall rock has undergone weak, diffuse silicification; however, it is not known whether the latter alteration was coeval with the chloritization or superimposed on it at a later time.

Mineralization and metal zoning

One of the most remarkable features of the San Rafael lode is the pronounced vertical zonation of the metals: copper being concentrated in the near surface parts of the deposit and tin dominantly at depth (Fig. 12). Above 4,975 m (i.e., near the surface), the lode averages < 1%

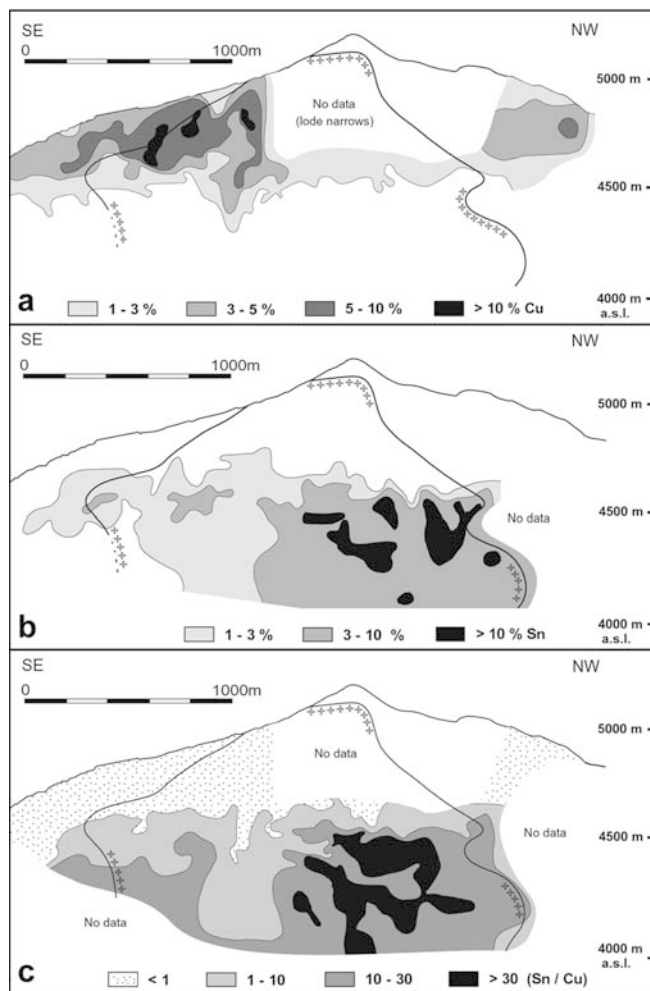


Fig. 12 Geochemical zoning in the San Rafael Lode (longitudinal section): **a** copper grades, **b** tin grades, **c** tin–copper ratios. All figures modified after Arenas (1999) and Minsur (unpublished data). The line with crosses indicates the limits of the granitoid stock

Sn and > 8% Cu. This changes to about 1% Sn and 4% Cu at the 4,600-m elevation and 1.5% Sn and 1.5% Cu at the 4,533-m elevation. Below the 4,533-m level, the average metal contents are 5% Sn and 0.2% Cu (Minsur, unpublished data). This zonation is very similar to that described from the Cornish tin deposits, such as the Dolcoath Main Lode (Taylor 1979; Clark et al. 1995). A vertical zonation is also evident in the style of mineralization at San Rafael. In the deepest parts of the deposit (3,900–4,450 m), the tin ore consists mainly of massive cassiterite; at higher levels (4,450–4,550 m), there is an interval of botryoidal wood tin; and in the massive chalcopyrite above the 4,550-m elevation, cassiterite occurs as the so-called needle tin variety.

Ores in the lower parts of the lode (below 4,533 m) generally have a simple mineralogy (quartz–chlorite–cassiterite, with minor wolframite and local chalcopyrite – Fig. 10d), whereas in the upper parts (above 4,533 m) they contain more diverse mineral associations involving quartz, chlorite, chalcopyrite, cassiterite, pyrrhotite,

arsenopyrite, pyrite, marcasite, sphalerite, galena, stannite, bismuthinite, native bismuth, calcite, fluorite and siderite. It is important to note that, whereas the tin orebodies are confined to the granitoid intrusion, copper orebodies straddle the contact between granitoid and slate or are located entirely within the metasedimentary rocks (Fig. 6a).

Figure 11 provides a simplified paragenesis for the San Rafael lode based on crosscutting relationships between different vein types. In chronological order, the principal vein types are:

1. Early, essentially barren tourmaline–quartz veins (with minor arsenopyrite).
2. Cassiterite (wood tin)–chlorite banded veins, veinlets and encrustations.
3. Cassiterite (massive)–quartz–chlorite-banded veins, some of which have cores comprising a late infill of quartz–chalcopyrite (with minor proportions of other sulfide minerals);
4. Chalcopyrite–cassiterite (needle tin)–quartz–chlorite veins (restricted to the upper part of the lode).
5. Quartz–chlorite–chalcopyrite–other sulfide minerals (e.g., pyrrhotite, pyrite, marcasite, sphalerite, galena) ± siderite, fluorite veins.
6. Late, barren quartz veins (with minor chlorite).
7. Late, barren carbonate- or fluorite-bearing veins (both types are relatively rare).

The different vein types listed above are associated with a variety of barren or mineralized breccias, which are cemented by tourmaline, chlorite, cassiterite, quartz, or sulfide minerals (Fig. 11). The breccias range from clast- to matrix-supported, and their clasts, which are angular or rounded, consist of fragments of chloritized, sericitized, or tourmalinized wall rock, as well as fragments of earlier veins and breccias. The lack of any fault gouge or tectonic fabrics suggests that these breccias are dominantly of hydrothermal origin.

Preliminary fluid inclusion studies

Microthermometric measurements have been conducted on fluid inclusions in quartz from a quartz–tourmaline vein (stage I), and in cassiterite and quartz from a banded cassiterite–chlorite–quartz vein (stage II). Primary fluid inclusions in the first sample generally contain liquid, vapor, and a halite crystal. They homogenize in the temperature range 460–510 °C, by disappearance of the vapor bubble or halite dissolution, and their salinity, estimated from the dissolution temperature of halite, ranges from 44–48 wt% NaCl eq.

The second sample is characterized by alternating layers (on a scale of millimeters) of cassiterite, chlorite, and quartz. Primary and pseudo-secondary fluid inclusions in cassiterite and primary inclusions in quartz are generally liquid-rich and in some cases contain an unidentified, tabular, birefringent solid, which does not

dissolve on being heated. This mineral is interpreted to be a trapped phase, possibly a phengitic mica. In addition, the quartz-hosted inclusions generally contain a tiny, opaque, nonmagnetic mineral, which is interpreted to be a daughter phase. Cassiterite-hosted primary and pseudo-secondary inclusions homogenize at a temperature of 355–360 °C, and, on the basis of the final ice melting temperature, are interpreted to have a salinity of 18–21 wt% NaCl eq. A temperature of initial ice melting (T_e) between –50 and –60 °C indicates that the fluid has a significant concentration of divalent cations. Quartz-hosted fluid inclusions homogenize at a temperature of 260–310 °C and have a salinity of 1–16 wt% NaCl eq.; T_e values are > –45 °C.

Discussion

Field relations at the San Rafael deposit indicate a strong structural control on tin mineralization. The bulk of the cassiterite ore is confined to large, high-grade orebodies, which are present only in the lower half of the San Rafael lode and are hosted entirely in granitoid rocks. The distribution of the tin orebodies was clearly controlled by several major fault jogs, which developed at depth in the lode during westward stepping of the sinistral–normal San Rafael fault. The creation of the fault jogs was limited to the mechanically competent granitoid host rock (as opposed to the incompetent slates that surround the pluton) and these dilational zones localized the formation of dense networks of tension fractures. The textures and the geometry of the spatially associated mineralized veins indicate that the hydrothermal activity was synkinematic and that the ore fluids were focused into these dilational sites.

Geologic evidence suggests that the ore veins were emplaced after the host intrusion had cooled appreciably and under a regional tectonic regime, as they are planar and cut straight across the granitoid contact (Sherlock 1999). This is consistent with geochronological data that indicate mineralization may have taken place 1–2 million years after emplacement of the intrusion. The latter was dated at 24.7 ± 0.3 Ma (Clark oral communication, 1997) by the U–Pb method on zircon and at 24.5 ± 0.7 Ma by the K–Ar method on biotite (Clark et al. 1983). By contrast, K–Ar dates of 23.6 ± 0.6 and 22.6 ± 0.5 Ma were obtained for hydrothermal muscovite (Kontak et al. 1987) and hydrothermal adularia (Clark et al. 1983), respectively. Similar brief time lags between cooling of igneous host rocks and tin deposition, have been reported from Bolivia (Grant et al. 1979), Cornwall, and Southern Thailand (Lehmann 1990).

The earliest hydrothermal event (Stage I) recorded in the San Rafael deposit is represented by numerous and volumetrically important tourmaline–quartz veins and breccia dykes, which clearly pre-dated ore deposition. On the basis of our preliminary fluid inclusion data, the fluids that produced the above veins and caused

pervasive, fracture-controlled sericitization and tourmalinization of the granitoids, were high temperature, hypersaline brines (460–510 °C, 44–48 wt% NaCl eq.). This early, barren tourmaline–quartz stage was marked by repetitive intense brecciation and, based on textural relationships, appears to have established the early framework of the San Rafael vein–breccia system, which was subsequently reactivated during the tin–copper event.

The main stages (II and III) of the hydrothermal system, during which tin and copper ores were deposited, were both characterized by strong chloritization, which overprinted the earlier alteration assemblages. This observation, the intimate association of needle tin cassiterite with chalcopyrite ores, and the uniform kinematics of the San Rafael lode throughout its history, all suggest that both tin and copper mineralization were introduced during a single, protracted hydrothermal event, albeit with copper being paragenetically later than tin. Petrographic relationships indicate that deposition of massive and wood tin cassiterite preceded that of chalcopyrite (and other sulfide minerals) and needle tin cassiterite.

It is still premature to propose a model that satisfactorily explains the genesis of the San Rafael deposit. However, some insights are provided by our preliminary fluid inclusion microthermometric data. These data indicate that the fluid trapped during the growth of cassiterite was of moderate salinity and at relatively high temperature (18–21 wt% NaCl eq., $T_h \sim 355\text{--}360$ °C), whereas that trapped by quartz had a lower, but much broader range in salinity and was at lower temperature (1–16 wt% NaCl eq., $T_h \sim 260\text{--}310$ °C). The trapping of two different fluids in separate cassiterite- and quartz-rich layers, millimeters in thickness, within the same vein implies that open fractures were periodically filled by one and then the other fluid. However, the broad range of salinity displayed by the quartz-hosted fluid inclusions also suggests that the two fluids mixed, which, considering their contrasts in temperature and composition, would have produced sharp gradients in physicochemical conditions, potentially favorable for cassiterite deposition.

Experimental studies have shown that in most hydrothermal solutions tin is transported in its reduced form, Sn (II), as the species SnCl_2° and SnCl^+ , and that cassiterite precipitation is induced by decreases in temperature and ligand ion activity (chloride) and increases in pH and fO_2 (Eugster and Wilson 1985; Pabalan 1986; Wilson and Eugster 1990; Taylor and Wall 1993; Müller and Seward 2001). The fluid trapped in cassiterite at San Rafael, therefore, quite clearly has the characteristics needed to make it an ideal ore fluid. The high temperature and salinity suggest that it was magmatic, which, considering the S-type character of the San Rafael pluton, implies that it was probably also reducing. Thus, the combination of high temperature, high salinity and low fO_2 would have made it a suitable fluid for tin transport. The second fluid, i.e., that trapped by quartz, which may

have had a salinity as low as 1 wt% NaCl eq., was likely of meteoric origin and, therefore, probably quite oxidizing, assuming a short residence time in the overlying strata. Mixing of the ore fluid with cool, dilute and relatively oxidizing meteoric water would have produced sharp decreases in temperature and ligand activity (Cl^-) and a sharp increase in fO_2 , all of which would have favored cassiterite precipitation. The rapidity with which these changes would have occurred in a mixing regime, characterized by repeated dominance of one fluid and then the other, would also have promoted supersaturation of SnO_2 , which could explain the high grade of the San Rafael ores. It would also explain the formation of the wood tin ores, which display colloform textures akin to those interpreted by Roedder (1968) and Hosking et al. (1987) as having formed in response to high nucleation rates, resulting from extreme supersaturation of the ore solutions.

Although more data need to be collected and geochemical modeling has to be undertaken in order to evaluate alternative hypotheses for the genesis of the San Rafael deposit (e.g., boiling, fluid–rock interaction, redox-coupled precipitation), the available information suggests a tentative working model, which explains many features of the orebodies. This model envisages that reducing fluids of dominantly magmatic origin extracted tin from the magma and transported it as Sn(II) chloride complexes to the site of deposition. Dilational zones created along the San Rafael fault by tectonic activity, synchronous with the hydrothermal processes, provided an effective mechanism for mixing these fluids with cooler, oxidized fluids of shallow meteoric origin. The ensuing rapid oxidation, cooling and dilution of ligand concentration in the ore fluid resulted in destabilization of the tin complexes and massive deposition of cassiterite in the open spaces provided by the fault jogs.

An additional and striking feature of the San Rafael deposit, which needs to be explained by any viable genetic model, is its marked, vertical primary metal zoning. The vast majority of the oxide (Sn) ores are hosted by fault jogs located at depth in the lode and confined to the intrusion. On the other hand, the sulfide (Cu–Zn–Pb) orebodies are mainly located on the upper flanks of the San Rafael vein–breccia system, where they straddle the metasedimentary rock–intrusion contacts or are contained entirely within metasedimentary rocks (Fig. 6). This apparent lithological control has also been documented for lode tin deposits elsewhere, e.g., the South Crofty deposit in Cornwall, where the mineralogy of the no. 9 lode “changes from tin- to copper-rich in a space of inches as it leaves the granite and enters the overlying slates” (Taylor 1979). Although stable isotope, bulk chemical and more detailed fluid inclusion studies will be needed to quantitatively assess the controls of sulfide mineral precipitation, it is tentatively proposed that the copper ores at San Rafael formed in response to a decrease in fO_2 , which occurred when the orthomagmatic and/or meteoric fluids interacted with the surrounding slates. The vertical metal zonation of the deposit is,

therefore, thought to reflect early tin mineralization, localized proximally to source by a favorable structural regime (fault jogs), and later, distal copper mineralization, localized by a gradient in physicochemical conditions at the interface of the intrusion with metasedimentary host rocks.

Acknowledgements The authors thank Ing. Fausto Zavaleta Cruzado, General Manager of MINSUR S.A., Ing. Otto Velarde Junes and Ing. Luis Alva Florian, successive managers of the San Rafael mine, Ing. Julver Alvarez Romero, Ing. Pastor Luque Malagá, Ing. Ladislao Guillén Cardenas and Ing. Luis Santalla Medrano, mine geologists, and other mine staff for their helpful collaboration during the field work. Many thanks go also to Harold E. Waller and Nestor Roldan from EMINASA; Mario Arenas Figueroa, consulting geologist; as well as to James R. Clark and David Dolejs, for useful comments on an early version of the manuscript. Finally, we acknowledge constructive reviews by David I. Groves and Michael Solomon, as well as the suggestions and encouragement of Noel C. White.

References

- Arenas MJ (1980a) El distrito minero San Rafael, Puno – Estaño en el Peru. *Bol Soc Geol Peru* 66:1–11
- Arenas MJ (1980b) Mapa geológico superficial del Distrito Minero San Rafael, Puno. MINSUR Archives
- Arenas MJ (1999) Exploración y geología de la mina San Rafael, Puno. *Mineria* 260:10–31
- Chappell BW, White AJR (1974) Two contrasting granite types. *Pacific Geology* 8:173–174
- Clark AH, Palma VV, Archibald DA, Farrar E, Arenas MJ, Robertson RCR (1983) Occurrence and age of tin mineralization in the Cordillera Oriental, Southern Peru. *Econ Geol* 78:514–520
- Clark AH, Farrar E, Kontak DJ, Langridge RJ, Arenas Figueroa MJ, France LJ, McBride SL, Woodman PL, Wasteneys HA, Sandeman HA, Archibald DA (1990) Geologic and geochronologic constraints on the metallogenic evolution of the Andes of southeastern Peru. *Econ Geol* 85:1520–1583
- Clark AH, Chen Y, Sandeman HA, Farrar E, Hodgson MJ, Kontak DJ, Arenas MJ (1995) Two giants and their lairs: the South Crofty, Cornwall and San Rafael, Peru, tin (–copper) deposits. 34th Annual Conference of the Ussher Society, Cornwall, pp 6–7
- Claire HV, Minaya ER (1979) Mineralización de los Andes Bolivianos en relación con la Placa de Nazca. Program ERTS Servicio Geológico de Bolivia, Sensores Remotes 4, La Paz
- Eugster HP, Wilson GA (1985) Transport and deposition of ore-forming elements in hydrothermal systems associated with granites. In: Halls C (chairman) High heat production (HHP) granites, hydrothermal circulation and ore genesis. Institute of Mining and Metallurgy Conference, London, pp 87–98
- Evans AM (1993) Ore geology and industrial minerals – an introduction. Blackwell, Oxford
- Grant JN, Halls C, Avila Salinas W, Snelling NJ (1979) K–Ar ages of igneous rocks and mineralization in part of the Bolivian tin belt. *Econ Geol* 74:838–851
- Hosking KFG, Stanley GJ, Camm GS (1987) The occurrence, nature and genesis of wood tin in south-west England. *Trans R Geol Soc Cornwall* 21(4):153–212
- Kirkham RV, Sinclair WD (1995) Porphyry copper, gold, molybdenum, tungsten, tin, silver. In: Eckstrand OR, Sinclair WD, Thorpe RI (eds) *Geology of Canadian mineral deposit types*. *Geol Surv Can, Geol Can* 8:421–446
- Kontak DJ, Clark AH (1988) Exploration criteria for tin and tungsten mineralization in the Cordillera Oriental of south-eastern Peru. In: Taylor RP, Strong DF (eds) *Recent advances in the geology of granite-related mineral deposits*. Proc CIM Conference on Granite-Related Mineral Deposits. Can Inst Mining Metall Spec Vol 39:157–169
- Kontak DJ, Clark AH, Farrar E, Pearce TH, Strong DF, Baadsgaard H (1986) Petrogenesis of a Neogene shoshonite suite, Cerro Moromoroni, Puno, southeastern Peru. *Can Mineral* 24:117–135
- Kontak DJ, Clark AH, Farrar E, Archibald DA, Baadsgaard H (1987) Geochronological data for Tertiary granites of the southeast Peru segment of the Central Andean Tin Belt. *Econ Geol* 82:1611–1618
- Kontak DJ, Cumming GL, Krstic D, Clark AH, Farrar E (1990) Isotopic composition of lead in ore deposits of the Cordillera Oriental, southeastern Peru. *Econ Geol* 85:1584–1603
- Kontak DJ, Clark AH, Halter W, Williams-Jones A (1995) Metal concentration versus dispersal in the magmatic–hydrothermal environment: a case study contrasting low-grade (East Kemptville, Nova Scotia) and high-grade (San Rafael, Peru) Sn-base metal deposits. *Proceedings of the 2nd Giant Ore Deposits Workshop, Kingston, Ontario*, vol 2, pp 347–413
- Laubacher G (1978) Estudio geológico de la region norte del Lago Titicaca, vol 5. Inst Geol Minería, Peru
- Lehmann B (1979) Schichtgebundene Sn-Lagerstätten in der Cordillera Real, Bolivien. *Berlin Geowiss Abh A*(14)
- Lehmann B (1990) Metallogeny of tin. *Lecture notes in Earth sciences* 32. Springer, Berlin Heidelberg New York
- Müller B, Seward TM (2001) Spectrophotometric determination of the stability of tin (II) chloride complexes in aqueous solution up to 300 °C. *Geochim Cosmochim Acta* 65:4187–4199
- Okulitch AV (1999) Geological time chart. The national Earth science series geological atlas. *Geol Surv Canada, Open File* 3040
- Pabalan RT (1986) Solubility of cassiterite (SnO₂) in NaCl solutions from 200 °C–350 °C, with geologic applications. PhD Thesis, Pennsylvania State University
- Palma VV (1981) The San Rafael tin–copper deposit, Puno, SE Peru. MSc Thesis, Queen’s University, Kingston, Ontario
- Roedder E (1968) The noncolloidal origin of “colloform” textures in sphalerite ores. *Econ Geol* 63:451–471
- Sandeman HA, Clark AH, Farrar E (1995) An integrated tectonomagmatic model for the evolution of the southern Peruvian Andes (13–20°S) since 55 Ma. *Int Geol Rev* 37:1039–1073
- Sandeman HA, Clark AH, Farrar E, Arroyo-Pauca G (1996) A critical appraisal of the Cayoni Formation, Crucero Basin, southeastern Peru. *J S Am Earth Sci* 9:381–392
- Sherlock RL (1999) Structural framework of the San Rafael tin–copper deposit, Peru. Unpublished report for Inca Pacific Resources Inc
- Sinclair WD (1995) Vein-stockwork tin, tungsten. In: Eckstrand OR, Sinclair WD, Thorpe RI (eds) *Geology of Canadian mineral deposit types*. *Geol Surv Canada, Geol Can* 8:409–420
- Singer DA, Mosier DL, Menzie DW (1993) Digital grade and tonnage data for 50 types of mineral deposits, Macintosh version. USGS open-file report 93-0280, USGS, Reston, VA
- Taylor RG (1979) *Geology of tin deposits*. *Developments in economic geology*, vol 11. Elsevier, Amsterdam
- Taylor JR, Wall VJ (1993) Cassiterite solubility, tin speciation and transport in a magmatic aqueous phase. *Econ Geol* 88:437–460
- Wilson GA, Eugster HP (1990) Cassiterite solubility and tin speciation in supercritical chloride solutions. In: Spencer RJ, Chou-I-Ming (eds) *Fluid–mineral interactions; a tribute to H.P. Eugster*. *Geochem Soc Spec Publ* 2:179–195